

# Learnable Pulse Accumulation for On-Device Speech Recognition:

How Much Attention Do You Need?

Yakov Pyotr Shkolnikov  
yshkolni@gmail.com

March 2026

## Abstract

Self-attention scales quadratically with sequence length, limiting transformer-based speech models on edge devices. We introduce the Learnable Pulse Accumulator (LPA), an  $O(n)$  replacement that substitutes key-query dot products with learned gating functions: content-dependent rectangular pulses, periodic windows, and position-dependent basis functions. An MSE diagnostic sweep determines per-layer replacement difficulty and ordering. Replacing 8 of 12 wav2vec2-base layers yields 10.61% word error rate (WER) on LibriSpeech test-clean, +7.24 percentage points (pp) over the 3.37% baseline, with  $3.27\times$  speedup at 120 s audio on Apple M4 Pro via an optimized MLX inference path. Cross-domain validation on SepFormer speech enhancement shows all 16 intra-chunk attention layers can be replaced without collapse, suggesting the depth wall arises from linguistic computation rather than an LPA limitation. LPA’s near-binary gates at inference enable dense GPU computation with no CPU–GPU synchronization, and all operations map to mobile neural accelerators.

**Keywords** speech recognition, efficient inference, attention replacement, on-device ASR, linear complexity

## 1 Introduction

Self-attention Vaswani et al. (2017) computes pairwise interactions across all sequence positions, requiring  $O(n^2d)$  operations for sequence length  $n$  and hidden dimension  $d$ . In speech, 50 Hz frame rates produce thousands of frames per utterance. At these lengths, attention dominates memory at all durations and latency beyond  $\sim 20$  s of audio.

On mobile hardware, the problem is compounded. Neural accelerators such as Apple’s ANE and Qualcomm Hexagon achieve peak throughput on element-wise and convolution operations but lack efficient support for the dynamic  $n\times n$  matrix multiplications that attention requires. This forces GPU fallback and negates the accelerator’s power efficiency. An ASR model whose mixing operations are entirely accelerator-compatible could achieve an order-of-magnitude speedup on device.

We propose the **Learnable Pulse Accumulator (LPA)**, which replaces key-query matching with learned gating functions that define soft windows over the sequence. Three gate types capture complementary patterns. *Aperiodic* pulses handle content-dependent segmentation, *periodic* pulses for multi-scale rhythmic structure, and *positional* pulses for fixed structural biases. The computation uses only depthwise convolution, sigmoid gating, and weighted summation, all of which are accelerator-compatible operations (Fig. 1).

LPA is architecturally distinct from prior  $O(n)$  alternatives. Linear attention Katharopoulos et al. (2020) approximates the softmax kernel. State space models (SSMs) Gu and Dao (2023) use

recurrent state evolution. SummaryMixing Parcollet et al. (2024) uses mean pooling. LPA instead uses *explicit learned windows* where each pulse defines where to aggregate information, how wide to look, and at what periodicity to repeat.

We convert a pretrained wav2vec2-base model to LPA via progressive layer-by-layer replacement, developing the techniques essential for preserving quality. Our contributions:

1. An  $O(n)$  primitive, gated pulse accumulation, with three complementary gate types for sequence mixing.
2. An MSE diagnostic sweep that measures per-layer replacement difficulty and determines optimal replacement order, providing a practical recipe for converting any pretrained transformer.
3. A roofline analysis demonstrating that pulse count has negligible impact on single-sample inference because additional pulses on hard layers add negligible cost.
4. Inference benchmarks on consumer hardware showing  $3.27\times$  speedup at 120s via a fused MLX/Metal path, with linear scaling and full mobile accelerator compatibility.

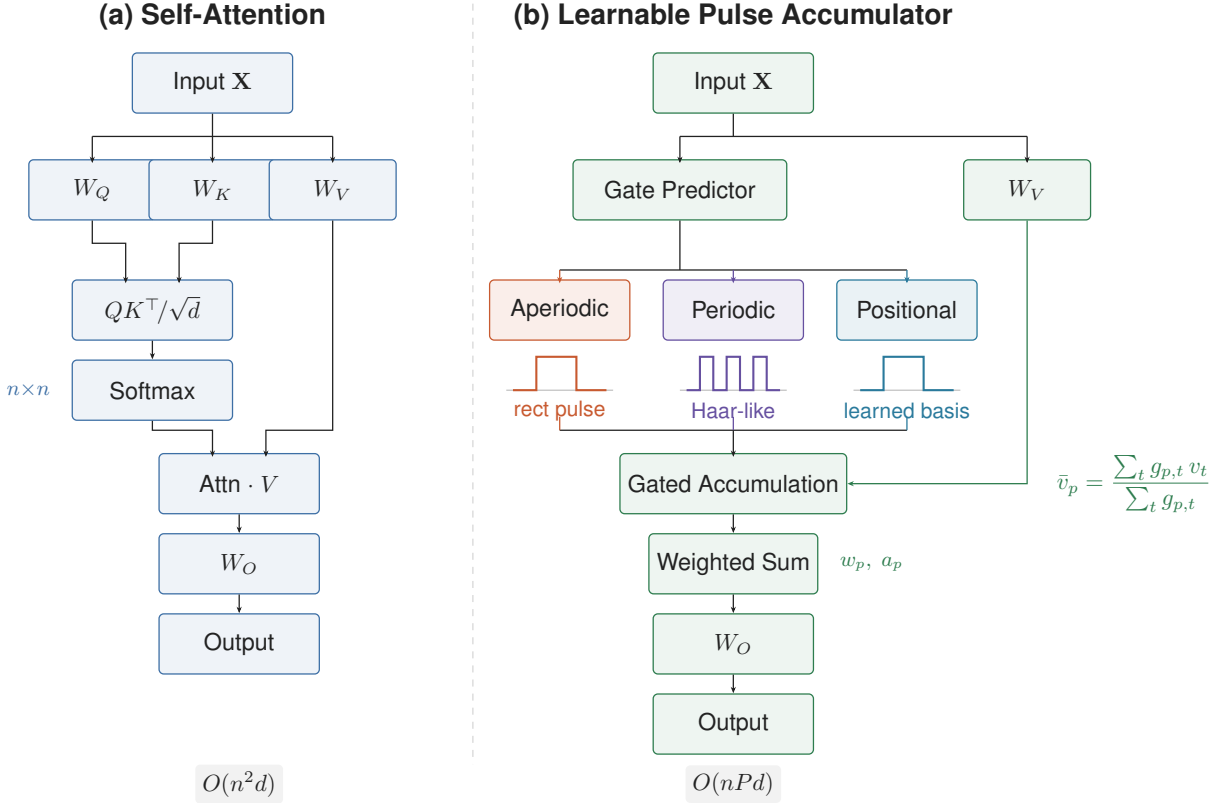
## 2 Related work

**Efficient attention and attention-free models.** Linear attention Katharopoulos et al. (2020) replaces the softmax kernel with a feature map ( $O(nd^2)$ ). Gated Linear Attention Yang et al. (2024) adds data-dependent forget gates with hardware-efficient chunkwise training. FlashAttention Dao et al. (2022) optimizes IO but retains  $O(n^2)$  complexity. The Attention Free Transformer (AFT) Zhai et al. (2021) replaces dot-product attention with element-wise sigmoid gating and learned position biases, but its full formulation retains  $T\times T$  position parameters and does not use explicit windowed accumulation. Mega Ma et al. (2023) combines exponential moving average with single-head gated attention, achieving linear complexity on long-range benchmarks. The Learnable Multi-Scale Wavelet Transformer Kiruluta et al. (2025) replaces dot-product attention with a learned Haar wavelet decomposition, achieving linear scaling on machine translation. These primarily target language modeling or general sequence tasks.

**Efficient speech models.** SummaryMixing Parcollet et al. (2024) replaces attention in wav2vec 2.0 with mean-pooling branches (18% faster, no quality drop on downstream tasks). The Polynomial Mixer Feillet et al. (2026) uses polynomial representations, outperforming SummaryMixing on LibriSpeech Panayotov et al. (2015). Fast Conformer Rekeshe et al. (2023) uses  $8\times$  downsampling for linear scaling (4.99% WER,  $2.8\times$  speedup). Zipformer Yao et al. (2024) uses a U-Net encoder with temporal downsampling, achieving faster inference than Conformer. LiteASR Kamahori et al. (2025) compresses Whisper via low-rank approximation of activations (50% encoder size reduction). Mamba-based approaches (ConMamba Jiang et al. (2025), Samba-ASR Shakhadri et al. (2025)) replace attention with SSMs but train from scratch on 10k+ hours.

**Progressive layer replacement.** LoLCATs Zhang et al. (2025) linearizes LLM attention via MSE distillation and LoRA. Mamba-in-the-Llama Wang et al. (2024) replaces attention with Mamba2 stepwise, finding end-to-end fine-tuning most impactful. GatedDeltaNet Yang et al. (2025) reports a 3:1 linear-to-attention ratio optimal in production (Qwen3-Next), consistent with our finding that 8/12 (2:1) LPA layers is the practical limit.

LPA differs from AFT and Mega in its use of *explicit square pulse windows* (aperiodic, periodic, positional) rather than global element-wise gating or exponential decay. Square pulses produce sparse, near-binary gate activations after temperature annealing, which both reduce arithmetic intensity and enable kernel fusion across consecutive LPA layers (the sparsity pattern is determined by a few gate parameters rather than a dense  $T\times T$  bias). LPA differs from SummaryMixing and LiteASR in replacing the mixing mechanism itself rather than using pooling or low-rank compression.



$P=12$  pulses,  $n=6,000$  (120 s audio):  
 Attention: 137 MB/layer vs. LPA: 281 KB/layer (**488×**)

Figure 1: (a) Standard self-attention computes an  $n \times n$  matrix via  $QK^\top$ . (b) LPA replaces this with three learned gate types that define soft windows over the sequence. Gated accumulation produces per-pulse summaries at  $O(nP)$  cost. All operations are accelerator-compatible.

The combination of gated pulse accumulation, speech/connectionist temporal classification (CTC) domain, and progressive replacement of pretrained attention is, to our knowledge, unexplored.

### 3 Learnable Pulse Accumulator

Given input  $\mathbf{X} \in \mathbb{R}^{n \times d}$ , LPA maintains  $P$  pulses, each with a gate  $g_p \in [0, 1]^n$  assigning soft membership to each position. The output at position  $t$  is

$$\text{LPA}(\mathbf{X})_t = W_O \frac{\sum_p w_p g_{p,t} a_p \bar{\mathbf{v}}_p}{\sum_p w_p g_{p,t}} \quad (1)$$

where  $w_p$  are softmax-normalized pulse weights,  $a_p$  are per-pulse amplitudes,  $W_O \in \mathbb{R}^{d \times d}$  is the output projection, and  $\bar{\mathbf{v}}_p$  is the gated mean of value-projected hidden states within pulse  $p$ . An active mask  $m_t = 1 - \exp(-\sum_p g_{p,t})$  suppresses output at positions with no gate coverage, applied as a multiplicative factor on the output:

$$\bar{\mathbf{v}}_p = \frac{\sum_t g_{p,t} \cdot W_V \mathbf{x}_t}{\sum_t g_{p,t}}, \quad W_V \in \mathbb{R}^{d \times d} \quad (2)$$

### 3.1 Gate types

**Aperiodic gates** predict center  $c_p$  and half-width  $\delta_p$  from the input via a learned query attention mechanism.

$$g_p^a(t) = \sigma\left(\frac{t-c_p+\delta_p}{\tau}\right) \cdot \sigma\left(\frac{c_p+\delta_p-t}{\tau}\right) \quad (3)$$

where  $\sigma(\cdot)$  denotes the sigmoid function,  $c_p = \sum_t t \cdot \text{softmax}(\mathbf{h}^\top \mathbf{q}_p / \tau)_t$  with  $\mathbf{h} = \text{MLP}(\text{DWConv}(\mathbf{X})) \in \mathbb{R}^{n \times d/2}$  (MLP = multi-layer perceptron, DWConv = depthwise convolution),  $\mathbf{q}_p \in \mathbb{R}^{d/2}$  is a learned query vector for pulse  $p$ , and  $\delta_p = \text{softplus}(f(\bar{\mathbf{h}}_p)) > 0$  ensures a valid interval, where  $\bar{\mathbf{h}}_p$  is the attention-weighted mean of  $\mathbf{h}$  using the same softmax weights as  $c_p$ . Temperature  $\tau$  anneals from soft to hard during training.

**Periodic gates** predict period  $T_p$ , phase  $\phi_p$ , and duty cycle  $d_p$ .

$$g_p^{\text{per}}(t) = \sigma\left(\frac{\cos(2\pi t/T_p - \phi_p) - \cos(\pi d_p)}{\tau}\right) \quad (4)$$

Period is parameterized as  $T_p = 2^{\text{softplus}(\cdot)+2}$  (minimum 4 frames), initialized across scales from  $\sim 10$  to 512 frames to capture phoneme-to-word-level repetitions.

**Positional gates** are content-independent. Each gate is a learned linear combination of  $K$  sin/cos basis functions over normalized position  $\hat{t} = t/(n-1)$ , passed through sigmoid:  $g_p^{\text{pos}}(t) = \sigma\left(\frac{\sum_{k=1}^K \alpha_{p,k} \sin(2\pi k \hat{t}) + \beta_{p,k} \cos(2\pi k \hat{t}) + b_p}{\tau}\right)$  where  $\alpha_{p,k}, \beta_{p,k} \in \mathbb{R}$  are learned coefficients and  $b_p$  is a bias. With  $K=16$  bases, these can represent arbitrary positional patterns including telegraph-like bi-level signals, capturing fixed structural biases that complement the content-dependent gates.

### 3.2 Architecture details

The aperiodic gate predictor uses a causal depthwise convolution (kernel 5) followed by a 2-layer MLP with GELU activation. Periodic and positional predictors use a single linear projection. Cross-layer coordination adds a projected summary of the previous LPA layer’s mean gate pattern as an additive bias. The value projection  $W_V$  and output projection  $W_O$  are initialized from the original attention weights.

### 3.3 Complexity

Per-layer cost is  $O(nPd + nd^2)$  vs. attention’s  $O(n^2d + nd^2)$ . With  $P=12$  and  $n=6000$  (120s audio), gate memory is 281 KB vs. attention’s 137 MB, a  $500\times$  reduction. At batch size 1, the  $nd^2$  projections dominate and the  $nPd$  accumulation is memory-bandwidth-bound on the input tensor, making  $P$  effectively free (Appendix E).

## 4 Progressive replacement recipe

We replace attention layers in a pretrained wav2vec2-base-960h Baevski et al. (2020) (3.34% WER on dev-clean) one at a time, progressing from easiest to hardest. The full recipe (Algorithm 1) requires only two inputs: the pretrained model and a training set.

The sweep (Step 1) produces both a difficulty ordering and a per-layer pulse allocation, since elastic net regularization prunes unneeded pulses on easy layers while retaining capacity on hard ones.

Three techniques in Step 2 proved critical. *Selective initialization* from attention weights and layer norm unfreezing together account for  $-31.8$  pp (Table 1), the single largest gain. *FFN co-adaptation* (unfreezing at  $0.1\times$  lr) adds  $-1.5$  pp, since each layer’s FFN was co-trained with its original attention.

---

**Algorithm 1:** Progressive LPA replacement

---

**Input** : Pretrained model  $\mathcal{M}$  with  $L$  attention layers, training set  $\mathcal{D}$ , WER budget  $B$

**Output** : Partially-replaced model with  $k$  LPA layers

**Step 1: MSE diagnostic sweep**

**for each layer**  $\ell = 0, \dots, L-1$  **do**

- Replace layer  $\ell$  with overprovisioned LPA ( $P_{\text{sweep}}$  pulses)
- Train 2 epochs:  $\mathcal{L} = \text{MSE}(\text{LPA}(\mathbf{X}), \text{Attn}(\mathbf{X})) + \lambda_1 \|\mathbf{a}\|_1 + \lambda_2 \|\mathbf{a}\|_2^2$
- Record MSE (difficulty) and surviving pulse count
- Restore original attention

Sort layers by increasing MSE  $\rightarrow$  replacement order

**Step 2: Progressive replacement**

**for**  $i = 1, \dots, L$  **in sweep order do**

- Initialize LPA from attention weights ( $W_O, W_V$ , partial  $W_Q$ )
- MSE warm-start: 2 epochs against original attention output
- CTC training: 8 epochs with temperature annealing  $\tau: 3.0 \rightarrow 0.5$ 
  - Unfreeze FFN at  $0.1 \times \text{lr}$ , unfreeze layer norm
- Alignment: jointly fine-tune all LPA layers ( $\leq 5$  epochs,  $0.5 \times \text{lr}$ )
  - Re-anneal all LPA temperatures globally
  - Auto-revert if WER increases
- if** WER  $> B$  **then stop**

Final joint fine-tuning: 8 epochs at  $0.2 \times \text{lr}$

---

*Temperature curriculum* contributes  $-2.9$  pp: during per-stage training only the current layer anneals, while during alignment all LPA layers re-anneal globally, providing smoother gradients for cross-layer adaptation.

## 5 Experiments

**Model.** facebook/wav2vec2-base-960h (12 layers, 768 hidden, 95M params, 3.34% WER on dev-clean), the standard pretrained release fine-tuned with CTC on 960h of LibriSpeech Panayotov et al. (2015).

**Data.** LibriSpeech train-clean-100 (100h) for early ablations, train-clean-360 (360h) for final configurations. Evaluation on dev-clean (2,703 utterances), greedy CTC decoding without language model.

**LPA config.** Base: 4 aperiodic + 4 periodic + 4 positional = 12 pulses per layer, kernel size 5, deep gate predictor (2-layer MLP for aperiodic, single projection for periodic/positional), cross-layer coordination, value projection, output gate, 4 heads, position modulation, dynamic content-dependent pulse weights, and skip connections from 4 layers back. In the +Order configuration, sweep-derived allocations override pulse counts (up to 36 for hard layers). The +Architecture configuration uses a fixed override of  $8+8+8=24$  pulses for deep stages ( $\geq 9$ ).

**Training.** 8 epochs/stage at  $\text{lr } 5 \times 10^{-4}$  with 10% linear warmup (FFN at  $5 \times 10^{-5}$ ), up to 5 alignment epochs at  $2.5 \times 10^{-4}$  with auto-revert, 8 final epochs at  $10^{-4}$ . CTC loss uses mean reduction and infinite-loss zeroing. MSE sweep: 2 epochs/layer with  $\lambda_1=0.01$ ,  $\lambda_2=0.001$ ,  $\theta=0.1$ , floor  $f=4$ . AdamW, BF16 mixed precision, batch 48 on NVIDIA H100. Total training cost for the full 10-stage progressive replacement (including MSE sweep, per-stage training, alignment, and final

Table 1: Cumulative ablation at 8/12 layers replaced (dev-clean WER %). Each row adds one technique to the previous configuration. Rows marked † are estimated by correcting an early evaluation bug (−9.3pp uniform offset, Appendix B). The bottom three rows use the corrected evaluation directly.

Configuration	WER	$\Delta$
Naïve replacement†	58.33	—
+ Selective init, unfreeze LN†	26.50	−31.8
+ Inter-stage alignment†	16.18	−10.3
+ FFN co-adapt ( $0.1 \times lr$ )†	14.64	−1.5
+ Temperature curriculum†	11.72	−2.9
+ Periodic + positional gates	10.25	−1.5
+ Skip connections, multi-head, 360h data	9.77	−0.5
+ MSE-ordered replacement	<b>9.35</b>	−0.4

joint tuning) is  $\sim 4$  GPU-hours on H100.

## 5.1 Ablation

Table 1 isolates each technique at 8/12 layers, where differences are most pronounced.

**Negative results.** Doubling pulse count (8→16) and adding per-pulse width predictors provided no improvement because gate capacity is not the bottleneck. Restricting temperature annealing to only the newly-replaced layer (rather than globally) degraded performance by 3–5 pp, confirming the curriculum effect.

## 5.2 Replacement order matters more than method

The MSE sweep shows large variation in replacement difficulty: early layers (0–2) have MSE 50–60 $\times$  lower than the final layer, with a general acoustic-to-linguistic trend (Table 6 in Appendix). Fig. 2 shows the progressive WER trajectory across four configurations that cumulatively add training recipe improvements, architectural changes, and difficulty-informed ordering. The most controlled comparison (“+Architecture” vs. “+Order”) uses identical architectures, data (360h), and hyperparameters, differing only in layer replacement order. Deferring the hard layer 8 from position 3 to position 7 reduces 6/12 WER from 7.32% to 5.64% (−1.68 pp, 23% relative).

At 8/12, WER drops from 58.33% (naïve) to 9.35% (full recipe) on dev-clean, with 10.61% on test-clean and 27.10% on test-other (Table 8, Appendix). Test-clean tracks dev-clean within  $\sim 1$  pp at all depths.

## 5.3 The depth wall

All configurations degrade sharply beyond 8–9 replaced layers. The transition from 9/12 to 10/12 adds +13–20 pp depending on configuration. The MSE sweep explains this directly. The final layers are far harder to approximate. Layer 11 has MSE 60 $\times$  higher than layer 0 (0.370 vs. 0.006), and layer 10 is 15 $\times$  harder.

We hypothesize this reflects a transition from acoustic to linguistic computation across encoder depth (Sec. 7). The MSE difficulty trend broadly tracks this transition, though non-monotonically (layer 4 is harder than layers 7–9). For deployment, the wall defines a quality–speed tradeoff curve. The MSE sweep tells the practitioner which layers to replace and when to stop.

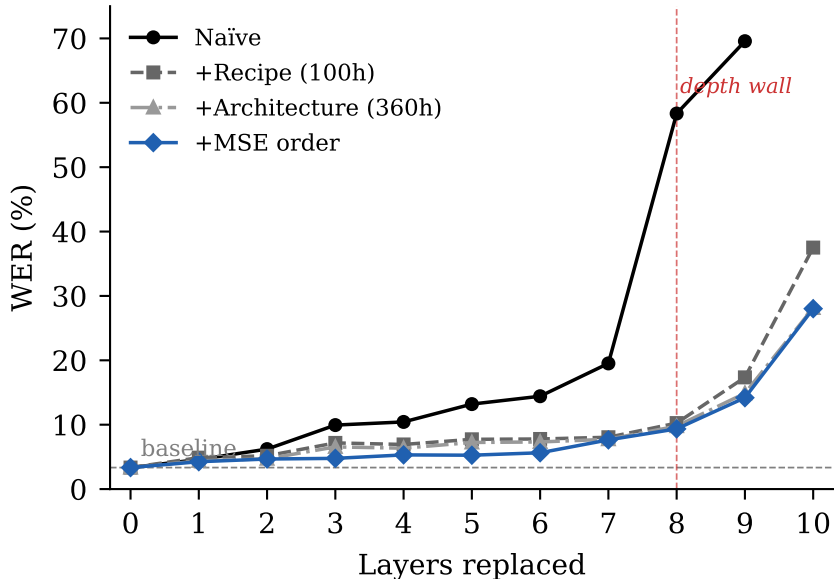


Figure 2: WER (%) vs. number of replaced layers across four cumulative configurations (full data in Table 7, Appendix). MSE-ordered replacement yields lower WER at every stage.

Table 2: SepFormer SI-SNRi (dB) on held-out test-clean during progressive LPA replacement of intra-chunk attention. All 16 layers are replaced without collapse.

Layers	SI-SNRi	$\Delta$ from baseline
0 (baseline)	5.69	—
2/16	8.89	+3.20
4/16	8.92	+3.23
8/16	8.14	+2.45
11/16	7.68	+1.99
16/16	6.82	+1.13

#### 5.4 Cross-domain validation: speech enhancement

To test whether the depth wall reflects linguistic computation requirements (as hypothesized) rather than an LPA architectural limitation, we apply the same progressive replacement recipe to SepFormer Subakan et al. (2021), a purely acoustic model for speech enhancement.

**Setup.** SepFormer-WHAM16k ( $\sim 26$ M params) uses a dual-path architecture with  $2 \times 8 = 16$  intra-chunk and  $2 \times 8 = 16$  inter-chunk attention layers (embed\_dim=256, 8 heads, chunk size  $K=250$ ). We replace the 16 *intra-chunk* layers progressively, using MSE-ordered replacement. The 16 inter-chunk (global) attention layers are retained. LPA uses 12 pulses per layer. Training and evaluation use LibriSpeech audio mixed with Gaussian noise at 5 dB SNR, with *separate* train (dev-clean, 2703 files) and held-out evaluation (test-clean, 2620 files) sets.

**Results.** Table 2 shows scale-invariant signal-to-noise ratio improvement (SI-SNRi, in dB) on the held-out set during progressive replacement.

**No depth wall appears.** All 16 layers are replaced, with every stage remaining above baseline. Performance peaks at 8.92 dB (4/16) and declines gently to 6.82 dB (16/16, still +1.13 above baseline),

Table 3: Inference time (ms) on Apple M4 Pro, batch size 1. *PyTorch*: MPS backend. *MLX*: Metal GPU, FP16 with FP32 accumulation. FP16 attention is slower than FP32 on MPS (the  $n \times n$  matmul does not benefit from half precision on this hardware), confirming that the MLX speedup reflects LPA’s algorithmic advantage.

Audio	Base (fp32)	Base (fp16)	8/12 (fp32)	12/12 (fp32)	8/12 (MLX)	Speedup vs fp16
10s	47	45	59	65	42	1.07×
30s	183	186	157	135	125	1.49×
60s	500	522	350	246	244	2.14×
120s	1668	1767	895	479	540	3.27×

whereas wav2vec2 collapses sharply at 8–9 layers. The MSE difficulty ratio across SepFormer layers is  $15\times$  (vs.  $60\times$  in wav2vec2), and difficulty does not correlate with depth, consistent with all layers performing acoustic rather than linguistic computation.

**Fine-tuning confound.** The improvement above baseline (5.69  $\rightarrow$  8.92 dB) is unexpected, since replacing attention with a lower-capacity mechanism should not improve performance. A control experiment that fine-tunes all 16 layers *with attention intact* using the same training budget reaches 11.34 dB, confirming that the improvement is primarily a fine-tuning effect (the pretrained checkpoint was trained on WHAM! noise, not Gaussian noise). The relevant comparison is therefore LPA (6.82 dB at 16/16) vs. fine-tuned attention (11.34 dB). LPA underperforms attention but does not collapse, which is the depth-wall finding.

**Caveats.** The evaluation uses Gaussian noise (simpler than WHAM!). SepFormer’s smaller embedding (256 vs. 768) means FFN layers dominate compute, so overall model speedup is only  $\sim 1.23\times$ . The value of the SepFormer experiment is the depth-wall validation, not raw speedup.

## 5.5 Inference speed

In the PyTorch/MPS reference implementation, the crossover where LPA becomes faster than attention occurs at approximately 20s, because per-kernel dispatch overhead exceeds the quadratic cost saved at shorter durations. A dedicated MLX inference path (Sec. A), which computes all gate operations as dense GPU kernels in half precision (fp16) and avoids CPU–GPU synchronization, shifts this crossover to below 10s. At 10s, MLX LPA achieves  $1.07\times$  speedup over the FP16 attention baseline.

Speedup scales linearly with input length (Fig. 3) because the  $O(n)$  vs.  $O(n^2)$  gap widens indefinitely. At 120s, the real-time factor is 0.0045. At batch size 1, linear projections dominate LPA time, making pulse count effectively free: 12 $\rightarrow$ 36 pulses adds only 0.6% (Appendix E). All LPA operations (depthwise convolution, sigmoid, element-wise multiply, linear projection) are compatible with mobile neural accelerators. FlashAttention is unavailable on Apple MPS/Metal, so the  $O(n^2)$  baseline reflects the actual on-device cost.

## 6 Comparisons

**Comparison to SummaryMixing.** SummaryMixing Parcollet et al. (2024) replaces attention with mean-pooled summaries:  $\mathbf{s} = \text{Linear}(\text{mean}(\mathbf{X}))$ , broadcast and added to a local per-position projection. Both LPA and SummaryMixing are  $O(n \cdot d^2)$ , but LPA learns *temporal selectivity* (which positions contribute to each output) while SummaryMixing uses uniform averaging.

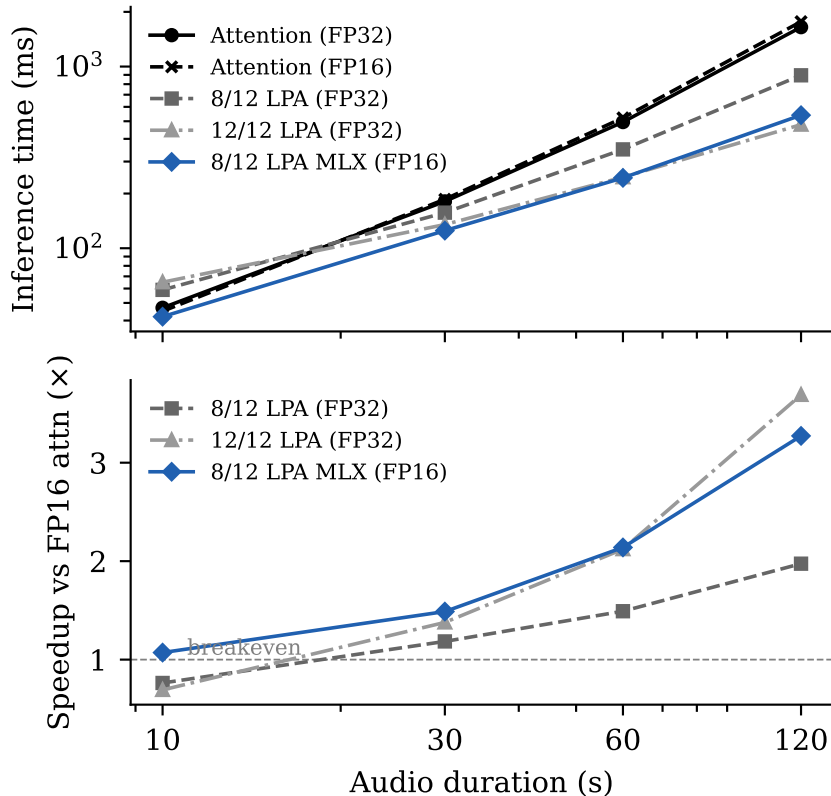


Figure 3: Speedup vs. FP16 attention baseline on Apple M4 Pro, batch 1. Top: inference time (ms, log scale). Bottom: speedup ratio. FP16 attention is slower than FP32 on MPS (Table 3).

Table 4 compares progressive replacement. On SepFormer, both methods use identical training budgets. On wav2vec2, the SummaryMixing implementation processes 2k samples per epoch (vs. LPA’s full  $\sim 28k$ ), giving LPA a training advantage that prevents direct comparison. Despite this caveat, the directional pattern is informative. LPA outperforms SummaryMixing at every wav2vec2 depth, with the gap widening from +1.2 pp at 1/12 to +9.1 pp at 4/12, while on SepFormer (where budgets are matched) SummaryMixing *matches or exceeds* LPA at all depths. This asymmetry is consistent with intra-chunk attention performing only local acoustic smoothing that mean pooling captures well, while wav2vec2’s linguistic layers require temporal selectivity.

**Comparison to Mamba-based ASR.** ConMamba Jiang et al. (2025) achieves 22.65% WER with 80h data. LPA at 8/12 achieves 10.61% with 360h fine-tuning, though the comparison is confounded by our pretrained wav2vec2 initialization vs. training from scratch. CALD He and Garner (2025) converts Wav2Vec2-*large* (317M params) attention to Mamba2 via layerwise distillation, achieving +0.32 pp WER on TED-LIUM. The comparison is not direct because CALD uses a  $3\times$  larger model with more redundancy, a different test set, and requires running the full attention model as a teacher during conversion. LPA operates on the smaller wav2vec2-base (95M params) without a teacher model, trading quality for a simpler, teacher-free conversion pipeline. Both approaches confirm that post-hoc attention conversion is viable for speech models.

**Quality gap in context.** At 8/12 replacement, LPA adds +7.24 pp over the 3.37% baseline, a meaningful degradation. Three factors suggest this gap is reducible rather than fundamental. First, the current recipe uses no distillation: each LPA layer is trained with CTC loss alone, while

Table 4: LPA vs. SummaryMixing (SM) progressive replacement. wav2vec2: dev-clean WER (%),  $\downarrow$ ). SepFormer: held-out test-clean SI-SNRi (dB,  $\uparrow$ , 16 intra-chunk layers). SepFormer uses identical training budgets; wav2vec2 SM uses fewer samples per epoch (see text).

Layers	wav2vec2 WER (%)		SepFormer SI-SNRi (dB)	
	LPA	SM	LPA	SM
0 (base)	3.18	3.18	5.69	5.69
1	4.26	5.44	7.27	8.38
2	4.64	7.31	8.89	9.60
4	6.38	15.47	8.92	9.62
8	9.92	29.04	8.14	9.12
16	—	—	6.82	7.88

CALD’s near-lossless result (+0.32 pp) and LoLCATs Zhang et al. (2025) both rely on per-layer MSE supervision from the original attention output as an auxiliary signal. Preliminary experiments with MSE auxiliary loss showed directional improvement but were confounded by simultaneous changes to replacement order. Second, the  $3.27\times$  speedup comes with 4 attention layers intact. GatedDeltaNet Yang et al. (2025) independently finds that a 3:1 linear-to-attention ratio is optimal in production (Qwen3-Next), suggesting that retaining a minority of attention layers for hard linguistic computation may be the right operating point rather than a limitation. Third, our hyperparameter search was limited: a single temperature schedule ( $\tau=3\rightarrow 0.5$ ), fixed learning rates, and no per-layer tuning of pulse allocation. Cross-layer skip connections (which proved important for depth  $\geq 9$ ) and per-head gate specialization were tested only in the final configuration. Systematic tuning of these choices remains unexplored.

## 7 Discussion: a new building block

Attention computes a data-dependent weighted average: the softmax of key-query dot products selects *which* positions contribute and *how much*. This is a matched filter, optimal when the target signal is buried in competing signals at unknown positions. But when the signal is spatially localized and spectrally distinct from noise, a simpler estimator suffices.

Consider a signal  $x(t) = s(t) + \eta(t)$  where  $s(t)$  is a target signal nonzero only on some interval  $[a, b]$  and  $\eta(t)$  is noise. The sufficient statistic for estimating  $s$  is the integral  $\int_a^b x(t) dt$ , uniform averaging over the support, with no weighting needed. The only information the estimator requires is the *support*  $[a, b]$  itself. This is what LPA’s gate predictor learns: where the relevant signal lives (center and half-width), not what it looks like (key-query match scores). The gate predictor replaces content matching with localization, and the rectangular window replaces softmax weighting with uniform integration.

Speech satisfies the localization premise. Phonemes occupy contiguous time intervals. Coarticulation effects span at most a few hundred milliseconds. The acoustic features at layers 0–7 of wav2vec2 are dominated by local spectro-temporal structure, the regime where gated integration extracts a sufficient statistic and the matched-filter machinery of attention is unnecessary. The MSE difficulty gradient quantifies this. Easy layers (MSE  $\sim 0.006$ ) have attention patterns that are already near-rectangular, while hard layers (MSE  $\sim 0.37$ ) have the content-dependent routing that rectangular windows cannot capture.

The three gate types cover complementary points on the Gabor time-frequency tradeoff Bao et al.

(2022); Wang et al. (2025): aperiodic gates provide temporal resolution, periodic gates track rhythmic structure, and positional gates supply fixed structural priors. The concurrent LMWT Kiruluta et al. (2025) applies a similar multi-resolution principle via learned Haar wavelets; LPA differs in using explicit rectangular pulses with learned centers and widths.

LPA returns to local processing but makes the receptive field *data-dependent*. The gate predictor uses a small depthwise convolution to predict where to look and how wide to integrate. The depth wall marks where this argument breaks down—wav2vec2’s deep layers perform linguistic computation that requires the content-dependent global routing attention provides. The SepFormer cross-validation, where all 16 intra-chunk layers are acoustic and all are replaceable, is the strongest evidence that the wall reflects the *nature of computation*, not an architectural ceiling. Further discussion of theoretical perspectives and open questions appears in Appendix F.

## 8 Limitations

The depth wall at 8–9/12 layers is the primary limitation. We have shown that it correlates with the acoustic–linguistic transition, but have not proven that LPA *cannot* perform linguistic computation. Different gate shapes or training from scratch might push the wall deeper. The SepFormer cross-validation supports the hypothesis but retains 16 inter-chunk attention layers as a confound. All wav2vec2 results are single-run without confidence intervals, though the consistent depth-wall pattern across four independent configurations (Table 7) provides implicit replication. All results use the same 95M-parameter model. Wav2vec2-large and Whisper are untested. The MLX speedup numbers (Table 3) combine LPA’s algorithmic  $O(n)$  advantage with the framework switch from PyTorch/MPS to MLX; all speedups use the FP16 attention baseline (see caption). LPA is complementary to distillation (which reduces model size) and quantization (which reduces precision). The three axes compose, and LPA’s element-wise operations are particularly amenable to low-bit quantization.

## 9 Conclusion

We introduced the Learnable Pulse Accumulator, a new  $O(n)$  building block for sequence mixing. LPA replaces key-query matching with learned gating functions (content-dependent rectangular pulses, periodic Haar-like windows, and position-dependent basis functions) that define where to aggregate information, how wide to look, and at what periodicity to repeat. We developed a practical conversion recipe. An MSE diagnostic sweep measures per-layer difficulty and determines replacement order, requiring no architecture search.

At 8/12 replacement, LPA achieves 10.61% WER on test-clean with  $3.27\times$  measured speedup at 120s audio on M4 Pro vs. an FP16 attention baseline, via a dedicated MLX inference path ( $1.97\times$  in the PyTorch/MPS path). The near-binary gate structure at inference enables dense GPU computation with no CPU–GPU synchronization, and all operations are compatible with mobile neural accelerators. Cross-domain validation on SepFormer speech enhancement confirms the depth wall is domain-specific. All 16 intra-chunk attention layers are replaced without collapse in a purely acoustic model, while wav2vec2’s linguistic layers resist replacement.

LPA is not a replacement for attention. It is a lower-cost primitive that works where attention is unnecessary, together with a recipe for determining where that boundary lies. Combining it with teacher distillation and hybrid architectures that retain attention only where needed could close the quality gap and bring efficient long-form ASR to mobile neural accelerators.

**Code availability.** Code and pretrained checkpoints will be released upon publication.

## References

- Alexei Baevski, Henry Zhou, Abdel-rahman Mohamed, and Michael Auli. wav2vec 2.0: A framework for self-supervised learning of speech representations. In *Advances in Neural Information Processing Systems (NeurIPS)*, 2020. arXiv:2006.11477.
- Chun Bao, Jie Cao, Yaqian Ning, Yang Cheng, and Qun Hao. Rega-net: Retina Gabor attention for deep convolutional neural networks. *arXiv preprint arXiv:2211.12698*, 2022.
- Tri Dao, Daniel Y. Fu, Stefano Ermon, Atri Rudra, and Christopher Ré. FlashAttention: Fast and memory-efficient exact attention with IO-awareness. In *Advances in Neural Information Processing Systems (NeurIPS)*, 2022. arXiv:2205.14135.
- Eva Feillet, Ryan Whetten, David Picard, and Alexandre Allauzen. Polynomial mixing for efficient self-supervised speech encoders. *arXiv preprint arXiv:2603.00683*, 2026. Accepted at ICASSP 2026.
- Albert Gu and Tri Dao. Mamba: Linear-time sequence modeling with selective state spaces. *arXiv preprint arXiv:2312.00752*, 2023.
- Mutian He and Philip N. Garner. Joint fine-tuning and conversion of pretrained speech and language models towards linear complexity. In *International Conference on Learning Representations (ICLR)*, 2025. arXiv:2410.06846.
- Xilin Jiang, Yinghao Aaron Li, Adrian N. Florea, Cong Han, and Nima Mesgarani. Speech slytherin: Examining the performance and efficiency of Mamba for speech separation, recognition, and synthesis. In *IEEE International Conference on Acoustics, Speech, and Signal Processing (ICASSP)*, 2025. doi: 10.1109/ICASSP49660.2025.10889391. arXiv:2407.09732.
- Keisuke Kamahori, Jungo Kasai, Noriyuki Kojima, and Baris Kasikci. LiteASR: Efficient automatic speech recognition with low-rank approximation. In *Conference on Empirical Methods in Natural Language Processing (EMNLP)*, 2025. arXiv:2502.20583.
- Angelos Katharopoulos, Apoorv Vyas, Nikolaos Pappas, and François Fleuret. Transformers are RNNs: Fast autoregressive transformers with linear attention. In *International Conference on Machine Learning (ICML)*, 2020. arXiv:2006.16236.
- Andrew Kiruluta, Priscilla Burity, and Samantha Williams. Learnable multi-scale wavelet transformer: A novel alternative to self-attention. *arXiv preprint arXiv:2504.08801*, 2025.
- Xuezhe Ma, Chunting Zhou, Xiang Kong, Junxian He, Liangke Gui, Graham Neubig, Jonathan May, and Luke Zettlemoyer. Mega: Moving average equipped gated attention. In *International Conference on Learning Representations (ICLR)*, 2023. arXiv:2209.10655.
- Vassil Panayotov, Guoguo Chen, Daniel Povey, and Sanjeev Khudanpur. Librispeech: An ASR corpus based on public domain audio books. In *Proc. IEEE International Conference on Acoustics, Speech and Signal Processing (ICASSP)*, pages 5206–5210, 2015. doi: 10.1109/ICASSP.2015.7178964.
- Titouan Parcollet, Rogier van Dalen, Shucong Zhang, and Sourav Bhattacharya. SummaryMixing: A linear-complexity alternative to self-attention for speech recognition and understanding. In *Proc. Interspeech*, pages 3460–3464, 2024. doi: 10.21437/Interspeech.2024-40.

- Dima Rekesh, Nithin Rao Koluguri, Samuel Kriman, Somshubra Majumdar, Vahid Noroozi, He Huang, Oleksii Hrinchuk, Krishna Puvvada, Ankur Kumar, Jagadeesh Balam, and Boris Ginsburg. Fast conformer with linearly scalable attention for efficient speech recognition. In *Proc. IEEE Automatic Speech Recognition and Understanding Workshop (ASRU)*, pages 1–8, 2023. doi: 10.1109/ASRU57964.2023.10389701.
- Syed Abdul Gaffar Shakhadri, Kruthika KR, and Kartik Basavaraj Angadi. Samba-ASR: State-of-the-art speech recognition leveraging structured state-space models. *arXiv preprint arXiv:2501.02832*, 2025.
- Cem Subakan, Mirco Ravanelli, Samuele Cornell, Mirko Bronzi, and Jianyuan Zhong. Attention is all you need in speech separation. In *IEEE International Conference on Acoustics, Speech, and Signal Processing (ICASSP)*, pages 21–25, 2021. doi: 10.1109/ICASSP39728.2021.9413901.
- Ashish Vaswani, Noam Shazeer, Niki Parmar, Jakob Uszkoreit, Llion Jones, Aidan N. Gomez, Lukasz Kaiser, and Illia Polosukhin. Attention is all you need. In *Advances in Neural Information Processing Systems (NeurIPS)*, 2017. arXiv:1706.03762.
- Junxiong Wang, Daniele Paliotta, Avner May, Alexander M. Rush, and Tri Dao. The mamba in the llama: Distilling and accelerating hybrid models. In *Advances in Neural Information Processing Systems (NeurIPS)*, 2024. arXiv:2408.15237.
- Zhen Wang, Shanshan Fu, Shuang Fu, Debao Li, Dandan Liu, Yexiang Yao, Haobo Yin, and Li Bai. Hybrid Gabor attention convolution and transformer interaction network with hierarchical monitoring mechanism for liver and tumor segmentation. *Scientific Reports*, 15(7454), 2025. doi: 10.1038/s41598-025-90151-8.
- Songlin Yang, Bailin Wang, Yikang Shen, Rameswar Panda, and Yoon Kim. Gated linear attention transformers with hardware-efficient training. In *International Conference on Machine Learning (ICML)*, 2024. arXiv:2312.06635.
- Songlin Yang, Jan Kautz, and Ali Hatamizadeh. Gated delta networks: Improving Mamba2 with delta rule. In *International Conference on Learning Representations (ICLR)*, 2025. arXiv:2412.06464.
- Zengwei Yao, Liyong Guo, Xiaoyu Yang, Wei Kang, Fangjun Kuang, Yifan Yang, Zengrui Jin, Long Lin, and Daniel Povey. Zipformer: A faster and better encoder for automatic speech recognition. In *International Conference on Learning Representations (ICLR)*, 2024. arXiv:2310.11230.
- Shuangfei Zhai, Walter Talbott, Nitish Srivastava, Chen Huang, Hanlin Goh, Ruixiang Zhang, and Josh Susskind. An attention free transformer. *arXiv preprint arXiv:2105.14103*, 2021.
- Michael Zhang, Simran Arora, Rahul Chalamala, Alan Wu, Benjamin Spector, Aaryan Singhal, Krithik Ramesh, and Christopher Ré. LoLCATs: On low-rank linearizing of large language models. In *International Conference on Learning Representations (ICLR)*, 2025. arXiv:2410.10254.

## A Edge Deployment: Fused Inference Kernels

A primary motivation for LPA is on-device speech recognition where quadratic attention is prohibitive. We describe an optimized inference path exploiting the structural properties of trained LPA gates.

### A.1 Hard gate inference

During training, gate temperature anneals from  $\tau = 3$  (soft) to  $\tau = 0.5$  (near-binary). At inference we set  $\tau \rightarrow 0$ , converting all gate computations to hard thresholds:

- **Aperiodic gates.** The softmax over  $T$  positions that finds each pulse center collapses to argmax. The sigmoid product  $\sigma\left(\frac{t-s_p}{\tau}\right)\sigma\left(\frac{e_p-t}{\tau}\right)$  (where  $s_p = c_p - \delta_p$  and  $e_p = c_p + \delta_p$  are the pulse start and end) becomes an indicator  $\mathbf{1}[s_p \leq t \leq e_p]$ . Each pulse selects a contiguous frame range.
- **Periodic gates.** The cosine-threshold gate  $\sigma\left(\frac{\cos\theta - \cos\pi d}{\tau}\right)$  becomes a step function. On-regions are determined analytically from the zero-crossings of  $\cos(2\pi t/p - \phi) - \cos(\pi d)$ , yielding  $\lceil T/p \rceil$  contiguous segments per pulse.
- **Learned-basis gates.** The sinusoidal basis  $\sigma(\mathbf{w}^\top \mathbf{f}(t)/\tau)$  thresholds to a binary mask, pre-computable for any sequence length  $T$  since the basis weights are content-independent.

This transformation is exact in the limit  $\tau \rightarrow 0$  and introduces no additional approximation beyond the training curriculum that already drives gates toward binary.

### A.2 Prefix-sum accumulation

With hard gates, the dense accumulation  $\mathbf{a}_p = \sum_t g_{tp} \mathbf{x}_t / \sum_t g_{tp}$  reduces to a range-sum. For each contiguous segment  $[s_i, e_i]$ :

$$\mathbf{a}_p = \frac{1}{|\mathcal{S}_p|} \sum_i (\mathbf{C}[e_i] - \mathbf{C}[s_i - 1]), \quad \mathbf{C}[t] = \sum_{t'=0}^t \mathbf{x}_{t'} \quad (5)$$

where  $\mathbf{C}$  is the prefix-sum of input features (computed once in  $O(TD)$ ), and  $|\mathcal{S}_p|$  is the total frame count across all segments. Pulse averages then require only  $O(P)$  indexed reads regardless of segment length.

The broadcast step is similarly sparse. At each position  $t$ , only pulses whose segments contain  $t$  contribute to the output. In practice, 3–5 of 12 pulses are active at any given frame.

### A.3 MLX implementation

We port the full Wav2Vec2 + LPA model to Apple’s MLX framework, computing all gate operations (convolution, MLP, argmax, thresholding) and accumulation/broadcast as dense GPU operations in fp16 with fp32 accumulation. This eliminates the CPU-GPU synchronization overhead inherent in PyTorch/MPS’s kernel dispatch model, where each LPA layer requires  $\sim 15$  separate kernel launches.

The main optimization is computing binary gates as dense tensors entirely on GPU, then using matrix multiplication for the accumulate step,  $\mathbf{S} = \mathbf{G}^\top \mathbf{X}$ , where  $\mathbf{G}$  is the  $[T \times P]$  binary gate matrix and  $\mathbf{X}$  is the  $[T \times D]$  input. Despite  $\mathbf{G}$  being binary, the dense matmul is faster than sparse alternatives at these dimensions ( $T \leq 6000$ ,  $P = 12$ ) because it avoids CPU-GPU round-trips for segment extraction.

For non-LPA encoder layers, we use MLX’s fused `scaled_dot_product_attention` kernel. The full model runs in fp16 with fp32 accumulation for numerical stability.

## A.4 Results

Table 5: Inference latency on Apple M4 Pro (36 GB, 273 GB/s), batch=1. 8/12 LPA layers replaced. *Speedup* relative to attention baseline. FP16 attention is slower than FP32 on MPS, so the precision-fair comparison favors LPA even more.

Audio	Attn (fp32)	Attn (fp16)	LPA (PT) (fp32)	LPA (MLX) (fp16)	Speedup vs fp16
10 s	47.1 ms	45.3 ms	58.8 ms	42.4 ms	1.07×
30 s	182.7 ms	186.1 ms	156.9 ms	124.9 ms	1.49×
60 s	499.7 ms	521.6 ms	349.5 ms	244.2 ms	2.14×
120 s	1668.0 ms	1767.1 ms	894.8 ms	540.1 ms	3.27×

The MLX LPA model achieves 3.27× speedup over the FP16 attention baseline at 120s and is 1.66× faster than the PyTorch MPS LPA path, confirming that LPA’s gate structure is amenable to framework-level optimization. At 120s, the real-time factor is 0.0045, well within real-time constraints for streaming speech recognition.

The hard-gate path introduces no measurable WER degradation: evaluation at  $\tau = 0.01$  vs  $\tau \rightarrow 0$  produces identical transcriptions on LibriSpeech dev-clean.

## A.5 Discussion

The speedup derives primarily from LPA’s  $O(n)$  gate structure replacing  $O(n^2)$  attention, providing increasing advantage at longer sequences (1.07× at 10s vs 3.27× at 120s). Running attention itself in fp16 on MPS is actually *slower* than fp32 (Table 5), because the  $n \times n$  attention matrix does not benefit from half precision on Apple Silicon at these sequence lengths. The framework switch from PyTorch/MPS to MLX contributes fused kernel dispatch, but the precision change does not inflate the reported speedup.

The structural sparsity of LPA gates (contiguous on-regions separated by off-regions) is not an incidental property but a direct consequence of the rectangular pulse parameterization. At inference, this binary gate structure enables the accumulation to be expressed as a simple matrix multiplication  $\mathbf{G}^\top \mathbf{X}$  with a sparse binary  $\mathbf{G}$ , requiring no special sparse kernels at the dimensions typical of speech ( $T \leq 7500$ ,  $P = 12$ ). For longer sequences where the dense matmul becomes expensive, a prefix-sum approach (Eq. 5) with a custom Metal kernel can reduce accumulation to  $O(P)$  indexed reads, though at these dimensions the CPU-GPU synchronization overhead of segment extraction outweighs the compute savings.

## B Evaluation Methodology

Early experiments used batched evaluation with naïve padding. The CTC decoder hallucinated predictions for padded regions, inflating all WER values by approximately 9 pp. The corrected evaluation uses per-sample output length computation to mask padding before CTC decoding. Training-time evaluation (10s audio filter) yields 3.34% on dev-clean. Full evaluation (30s filter) yields 3.18% on dev-clean and 3.37% on test-clean, matching the published 3.4%.

Later experiments use the corrected evaluation natively. For the Naïve column in Table 7 and the top rows (†) of Table 1, we apply a uniform  $-9.3$  pp offset to the inflated values from the early runs. This offset is approximate: the baseline correction is  $12.67\% \rightarrow 3.34\%$  ( $-9.33$  pp), and we verified that the corrected 8/12 result ( $10.25\%$ ) is within  $0.6$  pp of the offset-corrected estimate. These values should be treated as approximate.

## C Supplementary Tables

Table 6: Per-layer MSE difficulty from the elastic net diagnostic sweep. Layers sorted by increasing difficulty. The sweep overprovisions each layer with 144 pulses ( $12 \times 3$  types  $\times 4$  heads) and uses L1/L2 regularization to prune; the surviving count indicates how much capacity each layer demands. The MSE ranking determines replacement order (Sec. 5.2). The per-layer allocation suggested by the sweep has not been validated end-to-end (Appendix F).

Layer	MSE	Surviving / 144	Difficulty
L0	0.006	48	easy
L2	0.007	48	easy
L1	0.007	51	easy
L3	0.021	57	moderate
L6	0.030	74	moderate
L5	0.034	75	moderate
L7	0.043	87	hard
L8	0.046	100	hard
L9	0.052	87	hard
L4	0.065	89	hard
L10	0.096	96	very hard
L11	0.370	107	very hard

Table 7: Best WER (%) during progressive replacement. Columns show cumulative recipe improvements: training techniques (100h), architectural additions with 360h data, and deferred replacement order with MSE auxiliary loss. Naïve column estimated via uniform offset correction (Appendix B).

Layers	Naïve	+Recipe	+Architecture	+Order
0	3.34	3.34	3.34	3.34
1	4.59	4.88	4.38	<b>4.25</b>
2	6.21	5.17	4.71	<b>4.67</b>
3	9.94	7.17	6.55	<b>4.77</b>
4	10.43	6.93	6.35	<b>5.31</b>
5	13.20	7.73	7.24	<b>5.26</b>
6	14.42	7.78	7.32	<b>5.64</b>
7	19.52	8.05	7.74	<b>7.64</b>
8	58.33	10.25	9.77	<b>9.35</b>
9	69.57	17.35	14.88	<b>14.19</b>
10	—	37.51	28.13	<b>28.02</b>

Table 8: WER (%) across evaluation splits for the +Architecture configuration. All results use greedy CTC decoding without language model. Dev-clean baseline differs from Table 7 (3.18% vs. 3.34%) because this evaluation includes utterances up to 30s while training-time evaluation filters at 10s.

Layers	dev-clean	test-clean	test-other
0	3.18	3.37	8.67
1	4.26	4.63	11.83
2	4.64	4.78	12.67
4	6.38	6.62	16.52
6	7.35	7.90	18.98
7	7.90	8.50	20.84
8	9.92	10.61	27.10
9	15.82	16.56	37.08
10	30.39	31.62	54.51

## D Inference Benchmark Details

Full benchmark results on Apple M4 Pro, including per-configuration timing and memory estimates. PyTorch columns use MPS backend in FP32; MLX uses Metal GPU in FP16 with FP32 accumulation.

Table 9: Inference time (ms) across configurations and durations on Apple M4 Pro, batch 1. PT = PyTorch/MPS. MLX = MLX/Metal (FP16). Speedup is relative to the attention baseline (FP16).

Audio	Base (fp32)	Base (fp16)	8/12 (fp32)	12/12 (fp32)	8/12 (MLX)	Speedup vs Base fp16 12/12 PT	8/12 MLX
10s	47	45	59	65	42	0.69×	1.07×
30s	183	186	157	135	125	1.38×	1.49×
60s	500	522	350	246	244	2.12×	2.14×
120s	1668	1767	895	479	540	3.69×	3.27×

Table 10: Per-layer peak memory for gates/attention weights (float32).

Audio	Frames	Attention	LPA (12p)	Ratio
10s	500	0.95 MB	23 KB	42×
30s	1,500	8.6 MB	70 KB	125×
60s	3,000	34.3 MB	140 KB	250×
120s	6,000	137.3 MB	281 KB	500×

## E Roofline Analysis: Pulse Count at Batch Size 1

The MSE sweep allocates up to 36 pulses per layer for hard layers (vs. 12 base). A naïve FLOP analysis would suggest 3× slower LPA inference. A roofline analysis on M4 Pro (273 GB/s bandwidth, ~16.7 TFLOPS fp16) reveals this is wrong. At  $B=1$ , the LPA accumulation step is memory-bandwidth-bound, and the linear projections are near the compute-bandwidth crossover.

- **Attention** must read/write the  $n \times n$  score matrix per head. At  $T=6000$  with 12 heads, total score storage is 864 MB in FP16, the dominant cost.
- **LPA accumulation** reads the input tensor  $\mathbf{X} \in \mathbb{R}^{T \times D}$  once (18.4 MB at  $T=6000$  in FP32). The gate tensor  $\mathbf{G} \in \mathbb{R}^{T \times P}$  adds only  $P \times T \times 4$  bytes (864 KB at  $P=36$ ), just 4.7% of the input read.

Table 11: Roofline analysis: per-layer inference time ( $\mu\text{s}$ ) on M4 Pro,  $B=1$ ,  $T=6000$  (120s audio). Four  $768 \times 768$  linear projections dominate LPA time regardless of pulse count.

Component	Attention	LPA ( $P=12$ )	LPA ( $P=36$ )
Linear projections	1,696	1,696	1,696
$QK^\top$ / gate prediction	3,311	797	807
Softmax / element-wise	2,110	201	201
Scores $\times V$ / accumulation	3,311	136	142
<b>Total per layer</b>	<b>10,428</b>	<b>2,835</b>	<b>2,851</b>
<b><math>\times 12</math> layers</b>	<b>125 ms</b>	<b>34.0 ms</b>	<b>34.2 ms</b>

Going from 12 to 36 pulses costs  $+16 \mu\text{s}$  per layer ( $+0.2 \text{ ms}$  across 12 layers), a 0.6% increase. The four  $768 \times 768$  linear projections account for 60% of LPA time and are completely pulse-count-independent.

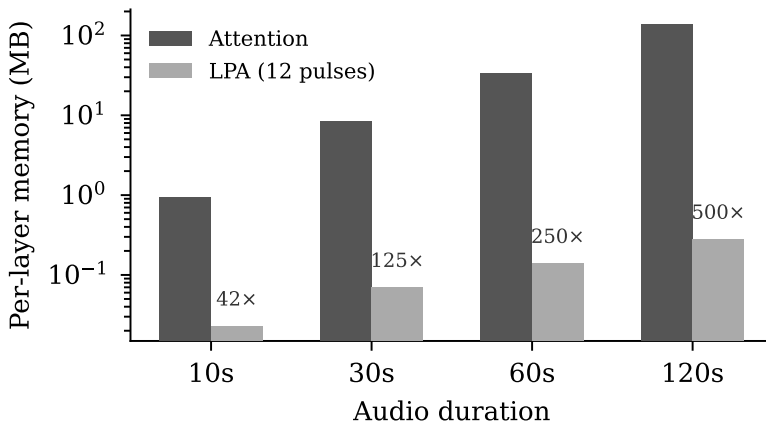


Figure 4: Per-layer memory for gates (LPA,  $P=12$ ) vs. attention score matrix across audio durations (FP32). LPA memory grows linearly while attention grows quadratically.

## F Theoretical Perspectives

### F.1 The local–global–learned-local circle

LPA’s intellectual lineage traces a circle in speech recognition architecture:

**Local** (1989): Time-Delay Neural Networks used shared weights across time with fixed local receptive fields.

**Global** (2017–present): Self-attention provided pairwise interactions across all positions, enabling arbitrary-range dependencies, but at  $O(n^2)$  cost.

**Learned-local** (this work): LPA returns to local processing but makes the receptive field data-dependent. The gate predictor uses a small depthwise convolution to predict where to look and how wide to integrate.

## F.2 Open questions

**Is the depth wall fundamental?** We have shown that the wall correlates with the acoustic-linguistic transition, but have not proven that LPA cannot perform linguistic computation. Different gate shapes or training from scratch might push the wall deeper.

**Fine-tuning confound.** The SepFormer control experiment (fine-tuning with attention intact: 11.34 dB vs. LPA’s 6.82 dB at 16/16) shows that improvement over the pretrained baseline is partly driven by continued training. Disentangling these effects requires matched-budget attention fine-tuning at each wav2vec2 stage.

**Training from scratch.** All experiments convert a pretrained attention model. The pretrained representations may be biased toward patterns attention can compute but LPA cannot. Samba-ASR’s success training Mamba from scratch (1.17% WER, 10K+ hours) suggests this is viable.

**Per-layer allocation.** The sweep suggests variable pulse allocation (Table 6), but all progressive results use fixed allocation. The sweep-derived allocation collapsed at 8/12 due to alignment instability, so its value is unvalidated.

**Generalization.** wav2vec2-large (317M, 24 layers) and Whisper are untested. Larger models may have more redundancy or more distributed representations.